

ION-BEAM PROPAGATION IN A LOW-DENSITY REACTOR CHAMBER FOR HEAVY-ION INERTIAL FUSION

D. A. Callahan

A. B. Langdon

Introduction

Heavy-ion fusion (HIF) is an attractive candidate for inertial fusion energy (IFE) production. In HIF, beams of heavy ions (mass ~ 100 to 200 amu) are accelerated and focused on an indirectly driven inertial confinement fusion (ICF) target. At the target, the ion energy is converted in a hohlraum into x rays, which implode the capsule. Accelerator drivers have the long lifetime (~ 30 years), high repetition rate (~ 5 Hz), and high efficiency ($\sim 30\%$) needed for commercial energy production. In addition, final focusing is accomplished via magnetic fields, which are not damaged by the blast.

The accelerator requirements are set by the target. In order to get efficient coupling of ion energy into x rays, the amount of radiator material in the target (Fig. 1) that needs to be heated must be kept reasonably small. Because the ions must be stopped in the target, the ion range (equal to the stopping distance times the material density) is related to the amount of material necessary. In order to keep the target mass reasonably small, an ion range ≤ 0.1 g/cm² is used. For ions of mass 100 to 200 amu, this corresponds to an ion energy of 3 to 10 GeV. To get the required beam power on target (5 to 10 MJ in 10 ns = $0.5\text{--}1.0 \times 10^{15}$ W), the beam current must be greater than 50 kA. This current is broken into several beams to keep the space-charge forces manageable. In

most conventional ion accelerators, space-charge plays only a small role; in a HIF accelerator, space-charge is very important.

The gain of a heavy-ion target generally increases as the size of the beam focal spot decreases. In order to get a small spot (radius ~ 2 to 5 mm), the beam emittance must be kept small. The beam emittance (a term used in accelerator physics) is proportional to the phase space area occupied by the beam and is related to the beam temperature. Keeping the emittance small throughout the accelerator in the presence of nonlinear fields (resulting from imperfect accelerator elements, misalignments, fringe fields, etc.) while performing the necessary beam manipulations (beam bending, beam combining, etc.) is a challenge. Recent *Quarterly* articles by W. M. Sharp¹ and A. Friedman² discuss issues and progress towards understanding the accelerator needed for a HIF power plant.

Once the beams leave the accelerator, they must be focused and transported through the reactor chamber to the target. Transporting the heavy-ion beams from the accelerator to the target is extremely important for a successful HIF reactor. Chamber transport (along with the target) sets the requirements on the accelerator driver.³ As a result, improvements in chamber transport and final focus can significantly reduce the cost of electricity. Relaxing the requirements on the accelerator reduces the cost of the driver, which directly impacts the cost of electricity; reducing the beam spot size at the target allows a larger target gain, which also reduces the cost of electricity. Improvements in beam transport and final focusing can be exploited in optimizing the end-to-end HIF system.

The main-line approach to chamber transport is low-density, ballistic or nearly ballistic transport. The HYLIFE-II reactor⁴ uses a low-density chamber with a pressure of a few millitorr. Even at the low density of the HYLIFE-II chamber (5×10^{13} cm⁻³ ≈ 0.003 torr), partial beam-charge neutralization is needed to overcome

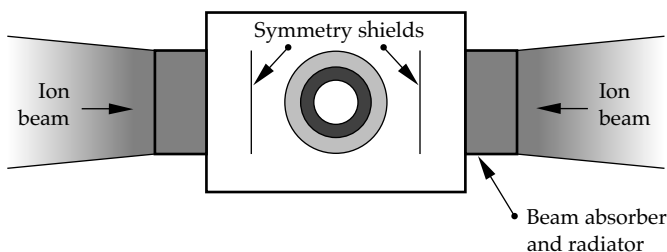


FIGURE 1. Schematic IFE heavy-ion indirect-drive target with end radiators. (40-00-1096-2401pb01)

the effects of beam stripping. In this case, beam stripping refers to collisional ionization of the beam ions to a higher charge state by the background gas. Beam stripping and neutralization have been recognized as important issues in chamber transport for many years.^{4,5} Low-density transport is the most conservative option, but puts strict requirements on the beam quality out of the accelerator.

In this article, we first discuss different effects that impact the beam spot size at the target. We then show that ballistic transport in a near vacuum is possible, but puts undesirable constraints on the reactor chamber design. We then discuss simulations of partially neutralized beam transport in a low-density chamber. Finally, we discuss calculations of multiple beam effects in the chamber. Partial neutralization allows chamber operation at higher pressures, and the use of ions with higher charge-to-mass ratio which are easier to accelerate. Both increases in flexibility allow for lower reactor cost.

Total Beam Spot Size at the Target

In this section we describe the different effects that lead to the final beam spot size at the target. The beam spot size is increased by the beam's space charge and emittance, chromatic aberrations in the final focusing system, and errors in aiming the beams at the target. These sources are roughly independent and add in quadrature,⁶

$$r_{\text{target}}^2 \approx r_s^2 + r_c^2 + r_a^2, \quad (1)$$

where r_{target} is the final spot radius at the target, and r_s , r_c , and r_a are the spot radius due to space charge and emittance, chromatic aberrations, and aiming, respectively. The simulation results presented in the sections below do not include chromatic aberrations or aiming errors; Eq. (1) is used to estimate the total spot radius. The spot radius necessary for a high gain (≥ 40) ranges from 2 to 6 mm depending on the details of the target design.

In the HYLIFE-II reactor concept, the targets are injected into the chamber at a rate of six per second using a gas gun. Petzoldt⁷ estimates that the spot radius due to errors in aiming the beams at the target is 0.4 mm. This estimate takes into account translational positioning errors and rotations of the target.

Chromatic aberrations occur in the final focusing system because particles with different longitudinal momenta are focused at different distances. This causes a radial spread in the particles at target, which is proportional to $\delta p/p$, the longitudinal momentum spread divided by the longitudinal momentum. For a focusing system of four thin lenses, single-particle calculations (neglecting space charge) show that $r_c = 8F\theta\delta p/p$, where F is the focal distance, and θ is the half convergence

angle of the beam. Including space charge reduces the chromatic aberrations by about a factor of 3/4, so

$$r_c \approx 6F\theta \frac{\delta p}{p}. \quad (2)$$

Generally F is set by the reactor geometry and has a value of ~ 5 m. The convergence angle θ is generally limited to ~ 15 mrad to avoid geometric aberrations in the final focusing magnets. It is possible to use larger angles and correct the geometric aberrations using an octupole correction.⁸ A larger convergence angle results in a larger aperture for the final focusing magnets, however, which increases the cost of those magnets. For the purposes of these calculations, we will keep $\theta \approx 15$ mrad.

Limiting the spot radius from chromatic aberrations to 1 to 1.5 mm sets a limit on the allowable momentum spread in the final focusing system. Using $F = 5$ m and $\theta = 15$ mrad, we find $\delta p/p \leq 2.2 - 3.3 \times 10^{-3}$ in the final focusing system. In the conventional HIF driver scenario, the beam is drift compressed by a factor of 10 or more between the end of the accelerator and the final focusing system. This is accomplished by giving the beam a velocity "tilt" so that the beam tail is moving faster than the beam head. After the tilt is applied, the beam is allowed to drift and it compresses as the tail catches up with the head. This drift compression increases the longitudinal momentum spread, and, as a result, $\delta p/p \leq 2.2 - 3.3 \times 10^{-4}$ at the end of the accelerator if the beam is to be drift-compressed by a factor of 10 prior to focusing.

If $r_a = 0.4$ mm, and $r_c = 1.5$ mm, then 2.57 mm are left for space charge and emittance (r_s) in a total spot (r_{target}) of 3 mm. An optimization needs be done to weigh the relative costs of each of the spot size contributions. We need to assess the cost of increasing $\delta p/p$ at the expense of beam emittance, for example.

The beam-spot radius from space charge and emittance can be estimated using the envelope equation

$$a'' = \frac{K}{a} + \frac{\epsilon^2}{a^3}, \quad (3)$$

where each ' indicates a derivative with respect to z , K is the perveance (which is a measure of the beam's space charge), ϵ is the unnormalized emittance, and a is the beam edge radius. Multiplying by a' and integrating gives

$$(\dot{a}_f)^2 - (\dot{a}_0)^2 = 2K \ln\left(\frac{a_f}{a_0}\right) - \epsilon^2 \left(\frac{1}{a_f^2} - \frac{1}{a_0^2}\right) \quad (4)$$

where 0 and f denote the initial and final values. At the beam waist $a_f = r_s$ and $\dot{a}_f = 0$. At the entrance,

$a'_0 = \theta$ and $a_0 \approx F\theta$. Using these substitutions and assuming $a_0 \gg r_s$, Eq. (4) becomes

$$\theta^2 = 2K \ln\left(\frac{a_0}{r_s}\right) + \frac{\varepsilon^2}{r_s^2}. \quad (5)$$

In the absence of space charge (i.e., a perfectly neutralized beam), $K = 0$ and the spot radius due to emittance r_e is given by

$$r_e = \frac{\varepsilon}{\theta}. \quad (6)$$

If $r_e = 1$ mm and $\theta = 15$ mrad, then transverse beam emittance is restricted to $\varepsilon \leq 15$ mm-mrad.

Using Eq. (5), we can estimate the maximum beam perveance allowed for a given r_s . Using $\theta = 15$ mrad, $a_0 = 7.5$ cm, $r_s = 2.5$ mm, and $\varepsilon = 15$ mm-mrad, Eq. (5) gives a maximum perveance of $K = 2.8 \times 10^{-5}$. The perveance is related to the beam current by

$$K = \frac{2Z}{(\gamma\beta)^3 A} \frac{I_b}{I_0}, \quad (7)$$

where Z is the ion charge state, β is the beam velocity over the speed of light, γ is the Lorentz factor, I_b is the beam current, A is the ion mass in amu, and $I_0 = m_{\text{amu}} c^3 / e = 31$ MA. For $K = 2.8 \times 10^{-5}$, this leads to a maximum current per beam of 2.3 kA for a mass-200 ion and 1.6 kA for a mass-135 ion, both at $\beta\gamma = 0.3$. Neutralization is needed if the current per beam is larger than these values.

Ballistic Transport in a Near Vacuum

Using the equations introduced in the previous section, we can show that a beam of 10-GeV, singly charged, heavy (~ 200 -amu) ions can be ballistically transported with a reasonable spot size provided the chamber density is low enough to avoid beam stripping. The target requires a main pulse with 4 MJ of energy in 10 ns (an additional 1 MJ is carried by a low-power prepulse). The total current necessary in the main pulse is $4 \text{ MJ} / (10 \text{ GeV} \times 10 \text{ ns}) = 40$ kA. Without neutralization, the maximum current per beam found in the previous section was 2.3 kA, so 17 beams are needed for the main pulse. This provides a reasonable, conservative scenario for transporting the beam to the target.

Beam stripping is an issue, however. Estimates of the cross section⁹⁻¹¹ for stripping the beam ions by the background gas in HYLIFE-II (BeF_2 from the

molten LiF-BeF_2 chamber wall) range from 1.3 to $4.0 \times 10^{-16} \text{ cm}^2$. Stripping only about 1% of the beam ions requires a chamber density $\approx 10^{11} \text{ cm}^{-3}$. This density is two orders of magnitude below the chamber density in the HYLIFE-II reactor ($\approx 5 \times 10^{13} \text{ cm}^{-3}$). Since a HIF reactor has a repetition rate of about 5 Hz, it is difficult to achieve densities lower than used in HYLIFE-II after each shot. Thus, purely ballistic transport puts an undesirable restriction on the chamber density.

Low-Density, Nearly Ballistic Transport

One option for improving the beam focus at the density of HYLIFE-II is to partially charge neutralize the beam. At the density of the HYLIFE-II chamber, the stripping mean-free-path is 0.5 to 1.5 m. In the HYLIFE-II design, the chamber radius from “first wall” to the target is 3 m (from target to the center of the last focusing magnets is about 5 m, as used in the “Total Beam Spot Size at the Target” section). Therefore, the beam will strip 2 to 6 times during chamber transport. Simulations with the BICrz code¹²⁻¹⁵ show that most of the stripped electrons tend to stay with the beam. However, in the higher charge state, the ions respond more strongly to the electric fields and the spot size increases. Simulations with a stripping mean-free-path of 1.2 m in a 3-m chamber show an increase in the beam spot radius from 2.6 mm (vacuum transport) to 8 mm. This is an unacceptably large spot, and partial beam neutralization must be used to offset this increase.

While beam stripping makes chamber propagation more difficult, ionization of the background gas by the beam ions can partially neutralize the beam and aid transport. Cross sections for collisional ionization of BeF_2 by the beam have a larger uncertainty than stripping cross sections because calculating molecular cross sections is more difficult than calculating atomic cross sections. Estimates of the mean-free-path for ionizing the background gas range from 0.7 to 25 m. For BeF_2 , the ratio of stripping to gas ionization cross sections is not favorable (i.e., more stripping than gas ionization). Other chamber gases, such as Li, may have a more favorable cross section ratio.¹⁶

Simulations show that including a stripping mean-free-path of 1.2 m and a gas ionization mean-free-path of 3.0 m reduced the spot radius from 8 to 5.4 mm. Neutralization by gas ionization occurs “for free” since we do not have to add anything to the reactor for it to occur; however, gas ionization neutralizes the beam slowly, so radial velocities develop before neutralization occurs. The solid

curve in Fig. 2 shows the neutralization fraction as a function of distance from the chamber wall for a simulation without beam stripping. The beam is more than 70% neutralized, but it takes about 2.5 m of propagation distance to reach this level of neutralization. To get a smaller spot, additional neutralization is needed.

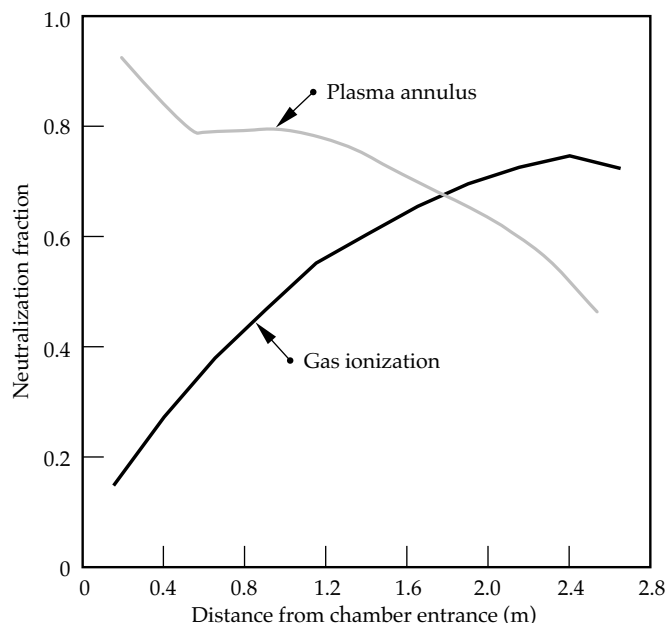


FIGURE 2. Neutralization fraction as a function of distance from the chamber entrance for neutralization using collisional ionization of the background gas (black curve) and neutralization using a preformed plasma annulus in the chamber (gray curve). (50-00-0696-1362pb01)

Neutralization Using a Preformed Plasma Annulus

Neutralizing an ion beam is more difficult than neutralizing an electron beam. When an electron beam passes through a plasma, the plasma electrons are moved out of the beam path, and the beam is neutralized by the immobile ions. For an ion beam, however, electrons must be pulled in from outside the beam path in order to reduce the net charge.

One method for neutralizing the beam quickly is to create a preformed plasma in the chamber before the beam enters. Simulations used a small ($0.3\text{-m} = 40\%$ of the beam length) annulus of plasma just inside the chamber entrance. A 4-kA beam of Pb^+ ions entered the chamber through the annulus. The annulus had a total electron charge of four times the beam charge.

As the beam entered the chamber, electrons were pulled from the inner surface of the annulus by the large radial electric field of the beam ($E_r = 16\text{ MV/m}$ at the beam edge for a 4-kA beam of radius 5 cm). The

electrons are accelerated longitudinally by the z electric field of the beam and oscillate back and forth across the beam in both the radial and longitudinal direction. The details of the acceleration and deceleration of the electrons in the longitudinal direction will depend on the shape of the beam. These simulations used a beam with a current profile that was parabolic in z .

Because the BICrz code is axisymmetric, particles cannot gain or lose angular momentum. The only angular momentum a particle has is the momentum it is created with. For the plasma annulus, we used an initial isotropic temperature of 100 eV. The particles can heat in r and z , but not in θ . As a result, a temperature anisotropy develops, which causes an excess of electrons near the axis. This causes the radial fields to become nonlinear. Figure 3 shows the radial velocity

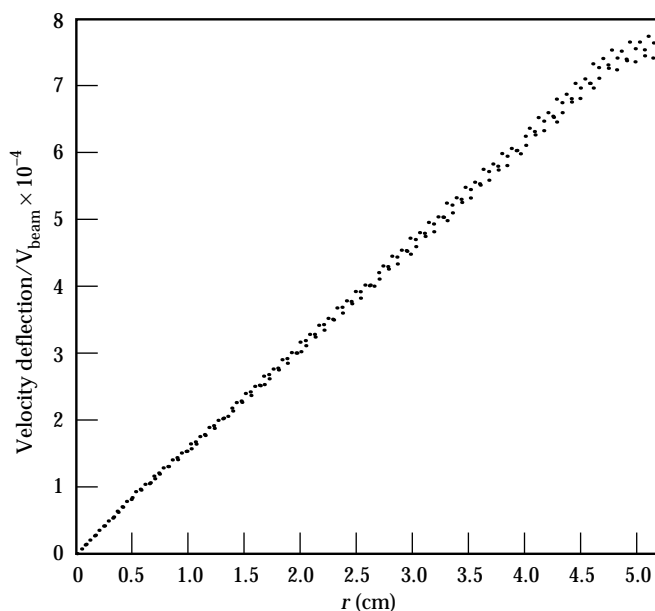


FIGURE 3. The radial velocity deflection of particles near the axial center of the beam as a function of radius shows the electric field is linear when no electrons are present. (50-00-0696-1363pb01)

deflection of particles near the center of the beam as a function of radius when no electrons are present. As expected, the field is linear. Figure 4 shows the same plot when the beam has passed through a plasma annulus (but with no beam stripping). The field is greatly reduced from the previous case, but the nonlinearity is also apparent. Because of the abundance of electrons near the axis, the field is negative at small radii. We can compensate for linear fields by increasing the focusing angle at the final optic. We cannot compensate for the nonlinear fields in this way; as a result the nonlinear fields can make it more difficult to focus the beam.

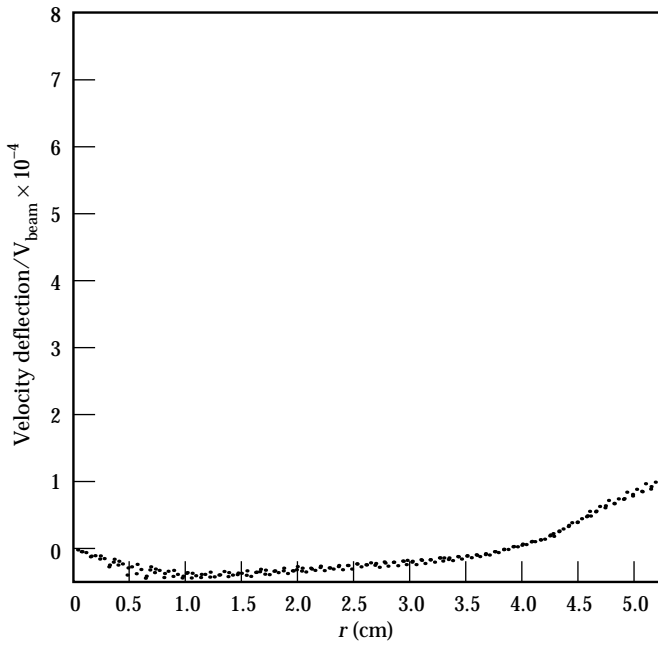


FIGURE 4. When electrons are present, the radial velocity deflection of particles near the axial center of the beam as a function of radius shows that the electric field is reduced, but nonlinear. (50-00-0696-1364pb01)

The charge neutralization fraction can be estimated using the Child–Langmuir space-charge-limited current from the inner surface of the annulus. For the 0.5-cm gap between the beam radius and the inner edge of the annulus used in this simulation, this estimate yields a neutralization fraction of 90%. Simulations are in agreement with this estimate, and the gray curve in Fig. 2 shows that the beam is quickly neutralized to slightly more than 90% while inside the annulus. As expected, neutralization reduces the beam spot size at the target. In a simulation with a stripping mean-free-path of 1.2 m and a plasma annulus, the final spot was 3.5 mm. This is a significant decrease over the 8-mm spot found without neutralization, but is not as good as the pure vacuum transport result of 2.6 mm.

The gray curve in Fig. 2 shows that while the beam is well neutralized near the chamber entrance, it does not remain well neutralized. The electrons pulled in from the plasma annulus are hot ($v_{th} \approx 0.3c$). As the beam compresses, the electrons do not compress as readily as the beam, and the neutralization fraction falls off as the beam approaches the target. The fact that these electrons are hot and as a result do not neutralize well near the target was seen in earlier studies.^{17,18} Electrons created by collisional ionization of the background gas are cooler than those pulled in from the plasma annulus, and we expect the smallest spot when both collisional ionization and a plasma annulus are included. Simulations confirm this, and the spot is reduced from 3.5 to 3.0 mm when a gas ionization mean-free-path of 3 m is added to the simulation.

Neutralization Using a Plasma Column

In the case of the plasma annulus, neutralization was quite good (>90%) inside the annulus, but the neutralizing electrons did not compress with the beam. As a result, neutralization got worse as the beam got closer to the target. One method to remedy this problem is to put the plasma throughout the entire chamber so the beam can continually pull in new electrons as it compresses.

The plasma density required in the plasma column is not large. Simulations show that ionizing just 0.44% of the background gas ($n_e = 2.5 \times 10^{11} \text{ cm}^{-3}$) in a cylinder of radius $\sqrt{2r_{\text{beam, initial}}}$ is enough to eliminate the effects of beam stripping when the stripping mean-free-path is 1.2 m. In this case, the electron density was six times the initial beam density. As the beam compressed, the beam density became much larger than the electron density.

One method for reducing the cost of the driver is to use a lighter, lower-energy ion such as 5.3-GeV Cs^+ . The cost of using the lighter, lower-energy ion is that more current is necessary to deliver the same energy to the target. For 5.3-GeV Cs^+ , 75 kA of current is needed to provide 4 MJ of energy in the 10-ns main pulse. We found in the second section that the maximum current we can transport in the chamber for a mass-135 ion without neutralization is 1.6 kA per beam. This means we would need more than 45 unneutralized Cs beams. With about 80% neutralization, we can transport the 75 kA of Cs in 10 beams.

In the simulation, the low-density plasma column neutralized the Cs beam quite well. A simulation with a 7.5-kA beam of 5.3-GeV Cs^+ ions (without beam stripping) and a low-density plasma column ($n_e = 2.3 \times 10^{11} \text{ cm}^{-3}$) produced a spot of 1.2 mm. This simulation used a smaller emittance (15 mm-mrad) than was used in some of the previous cases (33 mm-mrad). For these parameters, the unneutralized beam spot radius was 9 mm and the perfectly neutralized spot radius (from emittance only) was 0.9 mm. Figure 5 shows

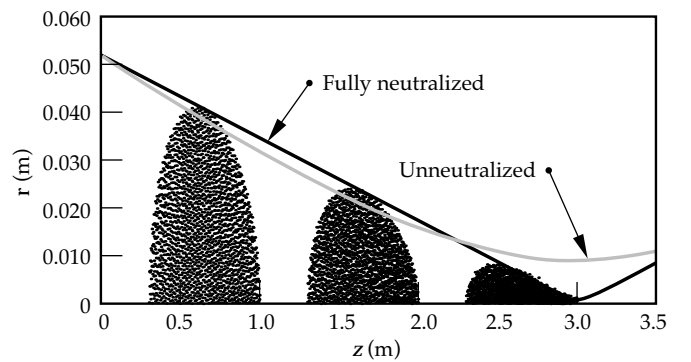


FIGURE 5. A particle-in-cell simulation shows that a 7.5-kA beam of 5.3-GeV Cs^+ ions is well neutralized by a low-density plasma column. The gray curve shows the envelope solution with no neutralization while the solid curve shows the envelope solution with perfect neutralization. (50-00-0696-1365pb01)

the simulation particles at three times plus the envelope solution for the unneutralized beam (gray curve) and the fully neutralized beam (black curve). The particles follow the fully neutralized envelope solution quite well indicating a high degree of neutralization.

Adding a beam stripping mean-free-path of 3.2 m to the Cs beam simulation produced a spot of 2 mm. This mean-free-path would correspond to a decrease of about a factor of two in the chamber density from the standard HYLIFE-II case.

Producing the plasma column in the HYLIFE-II chamber still needs to be addressed. Some methods under consideration are using an electrical discharge or a laser to ionize some of the chamber vapor and using a plasma gun to create the plasma and inject it in the chamber. Any equipment used to create the plasma (lenses, insulators, etc.) must be protected from the blast. This work is in progress.

Interactions Between Neighboring Beams

Most indirect-drive, HIF target designs have two radiation converters (one located at either end of the hohlraum). However, many beams (i.e., more than two) are necessary to reduce the space-charge forces. This means that half the beams will be aimed at each radiation converter, and these beams will be fairly close to one another in the chamber (see Fig. 6). As a result, each beam will be affected by the fields from neighboring beams, which can result in an increase in the beam spot size.

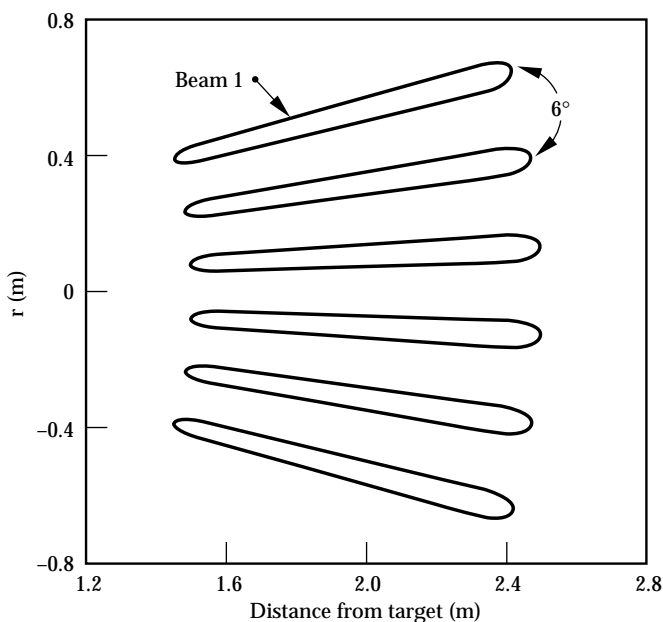


FIGURE 6. One option for multiple beam transport in the HYLIFE-II reactor is to place six beams in a “fan” aimed at one radiation converter. (50-00-0696-1366pb01)

If the fields due to the neighboring beams were constant along the beam length, we could compensate for them by increasing the focusing angle slightly. The fields are not constant, however, and vary along the pulse because of variations in the beam current as a function of z and the finite length of the beams. These two effects cause the field at the ends of the beam to be smaller than the field at the beam center. Since we cannot adjust the focusing angle on the time scale of the beam pulse duration (10 ns for the main pulse), the beam ends will be overfocused if the beam center is focused.

Hofmann, Hasse, and Reiser studied this problem for a cone of beams produced by an RF Linac with storage rings.¹⁹ In the RF Linac approach to HIF, beam compression is done by a phase rotation and results in a beam with a roughly Gaussian current profile. The variation in current along with the finite length of the beams causes a large variation in the electric field between the beam center and the beam ends. Hofmann et al. found that the increase in spot size due to the neighboring beams was tolerable for a charge state +1 beam, but scaled as the charge state squared, so that it was not acceptable for higher-charge-state ions.

This problem is less severe for beams produced by an induction linac. With careful longitudinal beam control, the induction linac can produce a nearly flat topped current pulse so that variations in the electric field come almost exclusively from the finite length of the beams. Calculations show $\leq 5\%$ beam loss for a “fan” of either six unneutralized, 4-kA beams of 10-GeV Pb^+ ions or six 70% neutralized, 7.5-kA beams of 5.3-GeV Cs^+ ions.²⁰

Complete simulations of the neighboring beams problem will require a fully three-dimensional, electromagnetic code. Such a code is under development by J.-L. Vay and C. Deutsch at University of Paris-Orsay.²¹

Summary

Transporting the heavy-ion beam through the reactor chamber to the target is a critical step in a HIF power plant. We have simulated low-density, nearly ballistic transport in a chamber that is consistent with the HYLIFE-II reactor design. Our simulations show that even at the relatively low densities of HYLIFE-II, beam stripping plays an important role. We have found that we can overcome the effects of beam stripping by charge neutralizing the beam using a low-density plasma column in the chamber.

Charge-neutralized transport has also opened up new accelerator regimes by allowing lower-mass, lower-energy ions to be used. Using lower-energy ions should reduce the cost of the accelerator driver, which in turn reduces the cost of electricity. Using

lower energy ions requires a larger beam current to deliver the same amount of energy to the target; transporting this large current requires either a very large number of beams or charge-neutralized transport. Our simulations showed that ionizing less than 0.5% of the background gas in the HYLIFE-II chamber is sufficient to transport a 7.5-kA beam of Cs^+ ions.

Experiments are needed to verify the results of the simulations. We believe that experiments to study beam neutralization can be done using existing facilities at LBNL or Sabre at Sandia National Laboratories.

Beam neutralization thus far has concentrated on "passive" neutralization using plasmas in the chamber. "Active" neutralization by co-injecting an electron beam along with the ion beam is another possibility for beam neutralization. Further study in this area is needed.

Notes and References

1. W. M. Sharp, *ICF Quarterly Report* 4(2), 70–77, Lawrence Livermore National Laboratory, UCRL-LR-105820-94-2 (1994).
2. A. Friedman et al., *ICF Quarterly Report* 5(3), 179–186, Lawrence Livermore National Laboratory, UCRL-LR-105821-95-3 (1995).
3. V. O. Brady, A. Faltens, D. Keefe, E. P. Lee, J. Hovingh, *Heavy Ion Fusion System Assessment: Final Focus and Transport Model*, LBL-23040, July 1987.
4. R. W. Moir et al., *Fusion Technology* 25, 5 (1994).
5. W. A. Barletta, W. M. Fawley, D. L. Judd, J. W.-K. Mark, and S. S. Yu, "Heavy-Ion Inertial Fusion, Interface between Target Gain, Accelerator Phase Space, and Reactor Transport Revisited," *Proc. of International Symposium of Heavy Ion Accelerators*, Tokyo, Japan, January 23–27, 1984 (UCRL-90246).
6. E. P. Lee, *Heavy Ion Inertial Fusion*, M. Reiser, T. Godlove, and R. Bangerter, Eds., *AIP Conference Proceedings*, American Institute of Physics, New York, NY, p. 461 (1986).
7. R. W. Petzoldt, Ph. D. Thesis, University of California at Davis, 1995.
8. D. D.-M. Ho, I. Haber, K. R. Crandall, S. T. Brandon, *Particle Accelerators* 36, 141 (1991).
9. N. Barboza, U.C. Berkeley, private communication (1994).
10. W. R. Meier et al., *Osiris and Sombro Inertial Confinement Fusion Power Plant Designs*, WJSA-92-01, DOE/ER/54100-1 (1992).
11. B. Badger et al., *HIBALL-2, An Improved Conceptual Heavy Ion Beam Driven Fusion Reactor Study*, UWFD-625, U. of Wisconsin (1984).
12. C. K. Birdsall and A. B. Langdon, *Plasma Physics via Computer Simulation*, McGraw-Hill, New York, 1985.
13. A. B. Langdon, *Computer Physics Communications* 70, 447 (1992).
14. A. B. Langdon, *Bull. Am. Phys. Soc.* 35, 2415 (1991).
15. D. A. Callahan and A. B. Langdon, *Proc. of the 1995 Particle Accelerator Conference*, pp. 3238–3240, Dallas, TX, May 1–5, 1995.
16. N. Barboza, submitted to *Fusion Engineering and Design*.
17. G. R. Magelssen and D. W. Forslund, *Heavy Ion Inertial Fusion, AIP Conference Proceedings*, p. 330, M. Reiser, T. Godlove, and R. Bangerter, Eds., American Institute of Physics, New York, NY (1986).
18. D. S. Lemons, M. E. Jones, *Heavy Ion Inertial Fusion*, M. Reiser, T. Godlove, and R. Bangerter, Eds., *AIP Conference Proceedings*, American Institute of Physics, New York, NY, p. 287 (1986).
19. I. Hofmann, R. W. Hasse, and M. Reiser, *J. Appl. Phys.* 73, 7061 (1993).
20. D. A. Callahan, *Appl. Phys. Lett.* 67, 27 (1995).
21. J.-L. Vay, accepted for publication in *Fusion Engineering and Design*.